ELSEVIER

Journal of Atmospheric and Solar-Terrestrial Physics 65 (2003) 1107–1116

Journal of ATMOSPHERIC AND SOLAR-TERRESTRIAL PHYSICS

www.elsevier.com/locate/jastp

Downward atmospheric longwave irradiance under clear and cloudy skies: Measurement and parameterization

M.G. Iziomon[a,*], H. Mayer[b], A. Matzarakis[b]

[a] *Department of Physics and Atmospheric Science, Dalhousie University, Halifax NS B3H 3JS, Canada*
[b] *Meteorological Institute, University of Freiburg, Freiburg, Germany*

Received 22 July 2002; received in revised form 14 May 2003; accepted 15 July 2003

Abstract

This paper evaluates models for the estimation of downward longwave atmospheric irradiance at a lowland location and a mountain location under clear and cloudy skies. The multiyear (1992–1995) data sets utilized for the study were recorded in southwest Germany during the REgio KLIma Projekt (REKLIP). Annual mean of downward atmospheric irradiance Ø↓ ranged from 315 to 328 W m^{-2} at the lowland site and from 282 to 290 W m^{-2} at the mountain site. Inter-annual variability of Ø↓ at the sites was less than 2%. Six existing downward longwave clear-sky irradiance models were assessed in this study. In addition, this study proposes a new parameterization for estimating downward longwave clear-sky irradiance at the surface. The new parameterization, which is validated with data from the Oklahoma-based U.S. Department of Energy Atmospheric Radiation Measurement (ARM) program, performed better than the other six models. It produced estimates, which agree with measurements more closely (within 5% for lowland and 7% for mountain locations). The incorporation of quadratic cloud terms in the parameterization allows for the estimation of Ø↓ under variable sky conditions.

Keywords: Downward atmospheric radiation models; Lowland; Mountain; REKLIP; ARM; Sky conditions

1. Introduction

Downward longwave atmospheric irradiance Ø↓ incident at the earth surface is a very significant constituent of the global radiation budget. Its knowledge is required for (a) the forecast of nocturnal frosts, fogs, temperature variation and cloudiness; (b) energy balance studies; (c) the design of radiant cooling systems as well as (d) calculations on climate variability and global warming (Crawford and Duchon, 1999; IPCC, 2001). However, current attempts to investigate energy balance at the earth's surface are still being hindered by lack of data on longwave fluxes (Garratt and Prata, 1996; Kessler and Jaeger, 1999). In view of this, there is a growing interest in alternative techniques for the estimation of longwave fluxes at the surface.

If the atmosphere is understood formally as a grey body, the amount of downwelling longwave irradiance is determined by the bulk emissivity ε_{atm} and effective temperature T_{atm} of the overlying atmosphere according to $Ø\downarrow = \varepsilon_{atm}\sigma(T_{atm})^4$, where σ denotes the Stefan-Boltzmann constant (5.67×10^{-8} W m^{-2} K^4). Since it is difficult to specify ε_{atm} and T_{atm} for a vertical column of the atmosphere (Crawford and Duchon, 1999), Ø↓ could be parameterized from air temperature T_a (K) and/or vapor pressure e (hPa) measured close to the ground, such that during clear-sky (with cloud cover $N = 0$ okta),

$$Ø\downarrow(0) = \varepsilon_0(T_a, e)\sigma T_a^4. \quad (1)$$

In Eq. (1), ε_0 (dimensionless) represents the effective clear-sky atmospheric emissivity.

* Corresponding author. Tel.: +1-902-494-1820; fax: +1-902-494-5191.

E-mail addresses: iziomon@mathstat.dal.ca (M.G. Iziomon), helmut.mayer@meteo.uni-freiburg.de (H. Mayer), andreas.matzarakis@meteo.uni-freiburg.de (A. Matzarakis).

1364-6826/$ - see front matter © 2003 Elsevier Ltd. All rights reserved.
doi:10.1016/j.jastp.2003.07.007

Ångström (1918) developed the first empirical relationship between downward longwave clear-sky irradiance and vapor pressure. Following his pioneering work, Brunt (1932), Swinbank (1963), Idso and Jackson (1969), Brutsaert (1975), Berger et al. (1984), Culf and Nash (1993), Alados-Arboledas (1993) and Prata (1996), among others, postulated additional models for the estimation of Ø↓ for clear-sky conditions. Crawford and Duchon (1999) estimated effective atmospheric emissivity for calculating daytime Ø↓ at Oklahoma. Chevallier et al. (2000) assessed the possibility of retrieving vertical profile of cooling rates and clear-sky Ø↓ from the Television and Infrared Observation Satellite (TIROS) Operational Vertical Sounder (TOVS) radiometers using a neural network approach, initialization inversion method and a forward radiative transfer model while Zhang et al. (2001) examined the impact of the atmospheric thickness on clear-sky Ø↓ in the Arctic and Subarctic.

Since there are still very few direct measurements of Ø↓, empirical models derived from surface measurements can provide many more estimates of Ø↓ than are currently available form observing networks. In addition, satellites have an inherent limitation in estimating Ø↓, because this quantity is effectively decoupled from the measurement, and not observable at all under overcast conditions (Prata, 1996). In view of their simplicity and practicability, empirical models (which estimates Ø↓ based on surface conditions) are generally preferred to theoretical models (which requires information on atmospheric properties including temperature and humidity at various levels above the ground). Consequently, one of the main objectives of this paper is to asses the applicability of some widely reported downward atmospheric irradiance models by using long-term surface data collected at a lowland site and a mountain site.

It is also noteworthy that most previous models are only valid for clear-sky or daytime conditions, while others are developed for estimating daily (or longer term) mean of Ø↓. These models are hence less accurate for estimating Ø↓ under cloudy conditions or within shorter time intervals. Some investigators (e.g. Czeplak and Kasten, 1987; Keding 1989; DIN-VDI, 1999) have parameterized the atmospheric downward irradiance in terms of cloud types. However, since information on cloud type is not as readily available as cloud cover fraction, the application of such parameterizations is somewhat limited. In view of the foregoing, another goal of this study is to develop a parameterization (based on easily measurable variables) for estimating Ø↓ under variable sky conditions for lowland and mountain locations.

2. Experimental sites and database

The reference sites used for this study are located at Bremgarten (47°54′35″N, 7°37′18″E) in the Upper Rhine plain and at Feldberg (47°52′31″N, 8°00′11″E) on the summit of the Black forest mountain ranges, southwest Germany. The experimental sites were operated within the framework of a regional climate project (REKLIP). Bremgarten lowland site is situated at an elevation of 212 m a.s.l. and Feldberg mountain site at 1489 m a.s.l.. The latter is located approximately 29 km southeast of the former. The surfaces of the experimental sites are grasslands.

Downward shortwave irradiance at the sites was measured by a horizontally positioned CM11 pyranometer (Kipp & Zonen, Delft, Netherlands) installed at 2 m above ground, while air temperature and humidity were measured using a wet and dry bulb psychrometer system at the same level. The total upward irradiance and total downward irradiance were measured, respectively, by the downward facing and the upward facing sensors of a horizontally positioned LXG055 pyrradiometer (B. Lange company, Berlin) installed at 2 m above ground. Downward atmospheric irradiance was computed as the difference between the total downward irradiance and the downward shortwave irradiance (Kessler and Jaeger, 1999). Prior to and after measurements, all radiometers were calibrated. There was no significant drift in the instruments' calibration constants at the end of the measurement period. The accuracy of the radiation measurements was generally estimated to be better than 5% especially during daytime conditions.

The data acquisition system was based on a Campbell scientific 21X micro data logger with 10 s sampling rate and 10 min integration time. Hourly mean values were determined from the integrated values. Measurement extended from January 1991 to September 1996 at the lowland site, and from July 1991 to September 1996 at the mountain site. However, it is worth-mentioning that the data set for 1994 at the mountain site was only restricted to the second half of the year, due to a storm-induced collapse of the measuring mast in the first half of 1994 at this site.

In addition to the aforementioned meteorological variables, which were directly measured at the study sites, hourly data on cloud cover for the mountain site (January 1991–October 1994) as well as data on sunshine duration for the mountain site (January 1991–October 1994) and lowland site (January 1991–February 1995) were obtained from the German Weather Service. Furthermore, hourly cloud cover data for the lowland site extending from January 1991 to February 1993 was obtained from the German Geophysical Consultant Services. The cloud cover fraction for the sites was determined by trained observers, who view the entire sky. Here a clear-sky implies the cloud cover fraction is 0 okta (i.e. no clouds).

3. Meteorological conditions at the experimental sites

From the point of view of climatic characteristic, the study sites lies in the transition area from maritime to continental climate, thus possessing a relatively mild and moderately

Table 1
Annual mean of meteorological parameters at Bremgarten lowland site and Feldberg mountain site, Germany (1992–1995)

Site	Air temperature (°C)	Vapor pressure (hPa)	Relative humidity (%)	Wind speed (m s^{-1})	Precipitation (mm yr^{-1})
Lowland	10.8	10.7	79.3	3.5	704
Mountain	4.4	7.4	84.1	6.7	1573

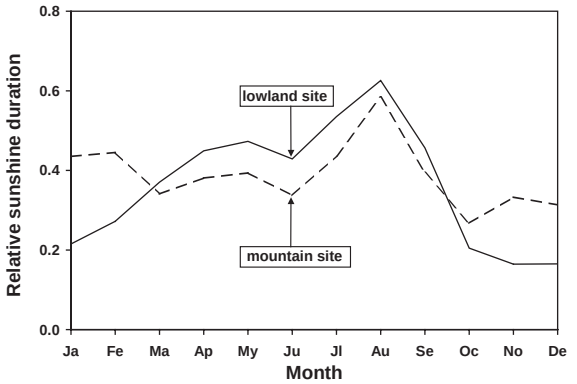

Fig. 1. Annual variation of relative sunshine duration at Bremgarten lowland site and Feldberg mountain site, Germany (1991–1994).

humid climate. Table 1 presents a summary of the annual mean of air temperature, vapor pressure, relative humidity, wind speed and precipitation at the sites from 1992 to 1995. These variables showed a strong dependence on site elevation. Unlike annual mean values of air temperature and vapor pressure, relative humidity (possibly owing to its inverse proportionality to air temperature) increased slightly with altitude in the study area. From 1992 to 1995, the absolute hourly minimum of air temperature was −13.1°C at the lowland site and −17.7°C at the mountain site, while the corresponding absolute maximum temperatures were 35.0°C and 23.8°C for the respective sites. On an annual basis, the mean number of days with cloud cover greater than 80% amounted to 104 at the lowland site and 112 at the mountain site, while the number of frosty days was 68 at the lowland site and 136 at the mountain site.

As shown in Fig. 1, the highest monthly mean relative sunshine duration S/S_0 (where S is the sunshine duration and S_0 is the day length i.e. maximum possible sunshine duration) was recorded in August at the study sites (being 62.5% for the lowland site and 58.5% for the mountain site), while the lowest monthly mean S/S_0 was recorded in November/December at the lowland site and October at the mountain site (been 16.5% and 27%, respectively).

4. Results and discussion

4.1. Measured downward atmospheric irradiance at the study sites

Fig. 2 presents annual variation of Ø↓ at the study sites. Monthly mean of downward atmospheric irradiance reached a maximum in July (when air temperature and vapor pressure peaked), being 367 W m^{-2} at the lowland site and 324 W m^{-2} at the mountain site. The least monthly mean of Ø↓ was recorded in January, being 289 W m^{-2} at the lowland site and 249 W m^{-2} at the mountain site. Annual means of Ø↓ at the study sites from 1992 to 1995 are presented in Table 2. Annual mean of Ø↓ for 1994 at the mountain site was omitted in Table 2 due to the incompleteness of the data set for this year at the site (see Section 2 above). The year-to-year fluctuation of Ø↓ was relatively small (less than 2%) at both sites. This low inter-annual variability of Ø↓ renders the measured data very suitable for diagnostic and modeling purposes. Overall, annual mean of Ø↓ ranged from 315 to 328 W m^{-2} at the lowland site and from 282 to 290 W m^{-2} at the mountain site. In effect, annual downward longwave radiation at the mountain site constituted 89% of that at the lowland site. This is consistent with the observed negative altitudinal temperature and vapor pressure gradient of −0.51°C/100 m and −0.25 hPa/100 m, respectively, for the study area.

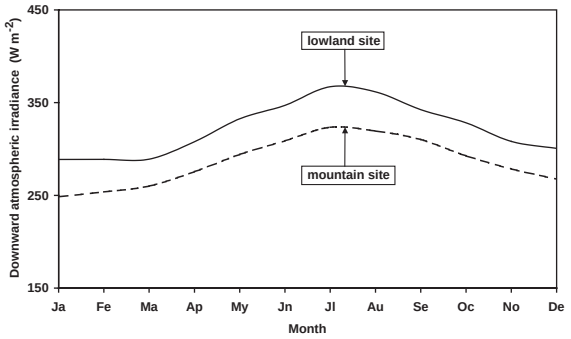

Fig. 2. Annual variation of atmospheric downward irradiance at the lowland site and mountain site (1992–1995).

Table 2
Annual mean and variability of downward atmospheric radiation at Bremgarten lowland site and Feldberg mountain site, Germany (1992–1995)

Site	Downward atmospheric radiation (W m^{-2})					Variability (%)
	1992	1993	1994	1995	Mean	
Lowland	315	319	328	324	322	1.9
Mountain	282	284	—	290	285	1.3

Table 3
Downward longwave clear-sky models and error analysis for estimated $Ø\downarrow(0)$ (obtained with the use of original model coefficients) at the lowland and mountain sites

Model	Definition of model	Errors associated with estimates	
	$Ø\downarrow$(W m^{-2}); T_a(K); e(hPa); $T_c = 273$ K	Lowland site	Mountain site
Swinbank1	$Ø\downarrow(0) = A_1 T_a^6$ where $A_1 = 5.3 \times 10^{-13}$ W m^{-2} K^{-6}	SE = 27 W m^{-2} NMBE = −7% NRMSE = 12%	SE = 29 W m^{-2} NMBE = 9% NRMSE = 15%
Swinbank2	$Ø\downarrow(0) = A_2 \sigma T_a^4 - B_2$ where $A_2 = 1.195$ and $B_2 = 171$ W m^{-2}	SE = 28 W m^{-2} NMBE = −11% NRMSE = 15%	SE = 29 W m^{-2} NMBE = 3% NRMSE = 13%
Idso and Jackson	$Ø\downarrow(0) = \sigma T_a^4(1 - A_3 \exp(-B_3(T_c - T_a)^2))$ where $A_3 = 0.261$ and $B_3 = 0.000777$ K^{-2}	SE = 27 W m^{-2} NMBE = −4% NRMSE = 11%	SE = 31 W m^{-2} NMBE = 1% NRMSE = 19%
Brunt	$Ø\downarrow(0) = \sigma T_a^4(A_4 + B_4 e^{1/2})$ where $A_4 = 0.55$ and $B_4 = 0.065$ $hPa^{-1/2}$	SE = 23 W m^{-2} NMBE = −6% NRMSE = 11%	SE = 24 W m^{-2} NMBE = 7% NMSE = 12%
ÅBF	$Ø\downarrow(0) = \sigma T_a^4(A_5 - (B_5 \times 10^{(-C_5 e)}))$ where $A_5 = 0.820$, $B_5 = 0.250$ and $C_5 = 0.168$ hPa^{-1}	SE = 27 W m^{-2} NMBE = 1% NRMSE = 9%	SE = 29 W m^{-2} NMBE = 2% NRMSE = 21%
Brutsaert	$Ø\downarrow(0) = A_6 \sigma T_a^4 e^{(1/7)}$ where $A_6 = 0.552$ $hPa^{6/7}$	SE = 23 W m^{-2} NMBE = −6% NRMSE = 10%	SE = 25 W m^{-2} NMBE = 7% NRMSE = 12%

4.2. Evaluation of downward atmospheric irradiance models

The assessment of downward atmospheric irradiance models would be examined in this section under three subdivisions namely (a) clear-sky condition: existing parameterizations, (b) clear-sky condition: a new parameterization, and (c) all-sky conditions.

4.2.1. Clear-sky condition: existing parameterizations

Based on model values calculated exactly according to the theory of radiative transfer, the equation of Swinbank (1963) (hereafter referred to as Swinbank1 model) has been reported to be one of the best approximation (DIN-VDI, 1999) for estimating downward atmospheric irradiance. Swinbank1 model (see definition in Table 3), which implies a quadratic relation between effective clear-sky atmospheric emissivity and T_a, is theoretically justified in terms of the 6.3 μm absorption band of water vapor (Llebot and Jorge, 1984).

In addition to Swinbank1, a second downward longwave clear-sky radiation parameterization (Swinbank2 model) proposed by Swinbank (1963), as well as four other widely reported models (Idso and Jackson, 1969; Brunt, 1932; Ångström, 1918/Bolz and Falkenberg, 1949 (ÅBF); Brutsaert, 1982) were evaluated for the study locations. Fig. 3 presents measured hourly values of $Ø\downarrow(0)$ and those estimated from the aforementioned models (using the original coefficients in Table 3) for a clear-sky summer day (30 August, 1991) at the lowland site. Although, there is strong autocorrelation in the hourly values of measured and estimated $Ø\downarrow(0)$, all the models underestimated $Ø\downarrow(0)$ for

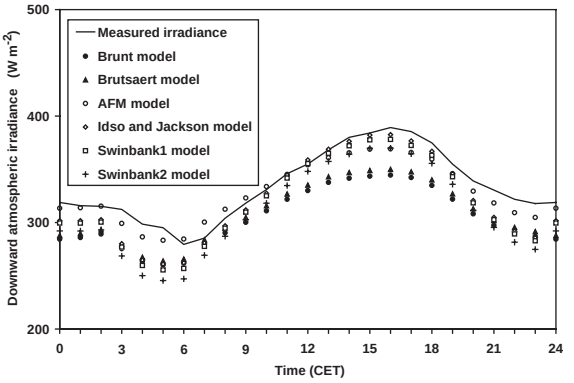

Fig. 3. Measured hourly downward atmospheric irradiance and those estimated from six different models on a clear summer day (30 August, 1991) at the lowland site.

most part of the day. In comparison to the remaining hours of the day, estimates from the models approached measured $\emptyset\downarrow(0)$ more closely during the second half of the morning, from 7 to 12 h (CET).

Moreover, the models were evaluated using all hourly clear-sky data from January 1991 to February 1993 (1633 hourly observations) for the lowland site and from August 1991 to October 1994 (1421 hourly observations) for the mountain site. Table 3 presents these models, as well as error statistics including the standard error (SE) in W m^{-2}, normalized mean bias error (NMBE) and normalized root mean square error (NRMSE). To obtain NMBE and NRMSE, the usual mean bias error and root mean square error are expressed as fractions of the corresponding mean $\emptyset\downarrow$. This current practice was also adopted during the major model testing activities performed by the Task IX of the International Energy Agency (IEA) (see Davies et al., 1988; Festa and Ratto, 1993; Badescu, 1997). Thus the SE, NMBE and NRMSE associated with hourly estimates of $\emptyset\downarrow$ from the models are given by

$$SE = \left[\left(\frac{1}{n(n-2)} \right) \left(n\sum_{i=1}^{n} (\phi\downarrow_{i,e})^2 - \left(\sum_{i=1}^{n} \phi\downarrow_{i,e} \right)^2 - \frac{\left[n\sum_{i=1}^{n} \phi\downarrow_{i,m}\phi\downarrow_{i,e} - \left(\sum_{i=1}^{n} \phi\downarrow_{i,m} \right) \left(\sum_{i=1}^{n} \phi\downarrow_{i,e} \right) \right]^2}{n\sum_{i=1}^{n} (\phi\downarrow_{i,m})^2 - \left(\sum_{i=1}^{n} \phi\downarrow_{i,m} \right)^2} \right) \right]^{0.5}, \quad (2)$$

$$NMBE = \frac{\sum_{i=1}^{n} (\phi\downarrow_{i,e} - \phi\downarrow_{i,m})}{\sum_{i=1}^{n} \phi\downarrow_{i,m}}, \quad (3)$$

$$NRMSE = \frac{\left[\frac{1}{n} \sum_{1}^{n} (\phi\downarrow_{i,e} - \phi\downarrow_{i,m})^2 \right]^{0.5}}{\frac{1}{n} \sum_{i=1}^{n} \phi\downarrow_{i,m}}, \quad (4)$$

where $\emptyset\downarrow_{i,m}$ and $\emptyset\downarrow_{i,e}$ are the ith measured and estimated downward atmospheric irradiance, respectively, and n is the number of data elements.

The standard error of $\emptyset\downarrow(0)$ estimated from the models, ranged from 23 to 28 W m^{-2} for the lowland site and from 24 to 31 W m^{-2} for the mountain site. While the NRMSE of hourly estimates of $\emptyset\downarrow(0)$ from Brutsaert, Idso and Jackson, Brunt and ÅBF models was $10 \pm 1\%$ for the lowland site, only Brutsaert and Brunt model yielded a relatively low NRMSE (of 12%) for the mountain site.

We also examined the linear correlation between model estimates and measurements, where the correlation coefficient for the perfect fit (with zero intercept) is denoted by r. Figs. 4 and 5 present plots of hourly estimates of $\emptyset\downarrow(0)$ from Idso and Jackson model, and Brutsaert model versus measured values for the lowland and mountain sites. As evident by the relatively low magnitude of their statistical errors (see Table 3) and high correlation coefficients ($r^2 \approx 0.78$ for the lowland site, $r^2 \approx 0.55$ for the mountain site) (see Figs. 4 and 5), Brunt and Brutsaert models performed better than the other models. In particular, Brutsaert model gave the highest correlation coefficient for both sites. Swinbank2 model yielded the worst SE for the lowland site, while Idso and Jackson model showed the worst SE for the mountain site (see Table 3 and Figs. 4 and 5). One notable observation about these comparisons is the shelf, below which model estimates seem not to occur (see Figs. 4 top, 5 top and 5 bottom). The lower accuracy of these models could be attributed to the fact that the models assumed that air humidity is an implicit function of ambient temperature (based on the strong correlation between T_a and e) and hence did not express e explicitly in their formulation.

Expressing Brunt model as $\varepsilon_0 = A_4 + B_4 e^{1/2}$ where the clear-sky emissivity $\varepsilon_0 = \emptyset\downarrow(0)/\sigma T_a^4$, Table 4 presents the coefficients A_4 and B_4 obtained from measured data for the study sites as well as those reported by some investigators. These coefficients vary somewhat significantly from location to location. In general, B_4 varied more than A_4, with the former showing a variability of about 32% and the latter only 13% for all the locations presented in Table 4. The estimated coefficient B_4 for the lowland and mountain sites are 0.064 and 0.066 respectively. The higher B_4 obtained for the mountain site implies a slightly greater dependence of the effective emissivity on the surface water vapor. While B_4 for the study sites is similar to that reported originally by Brunt (1932), A_4 for both sites differed significantly and showed a deviation of about 10% from that reported by Brunt (1932). With A_4 amounting to 0.60 at the lowland site and 0.50 at the mountain site, it follows that, given the same surface water vapor pressure at both sites, the emissivity is lower at the mountain site. Thus, the difference in A_4 for

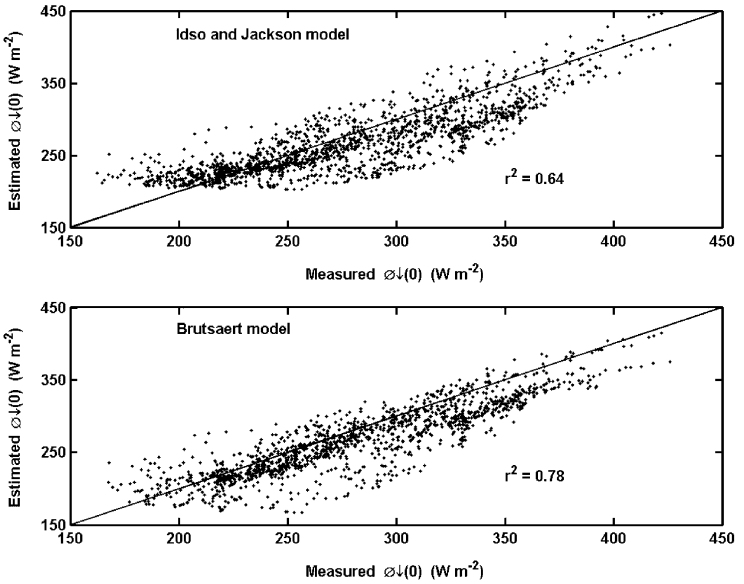

Fig. 4. Hourly downward longwave clear-sky irradiance estimated from Idso and Jackson (above) and Brutsaert (below) models versus measured irradiance at the lowland site (1991–1992).

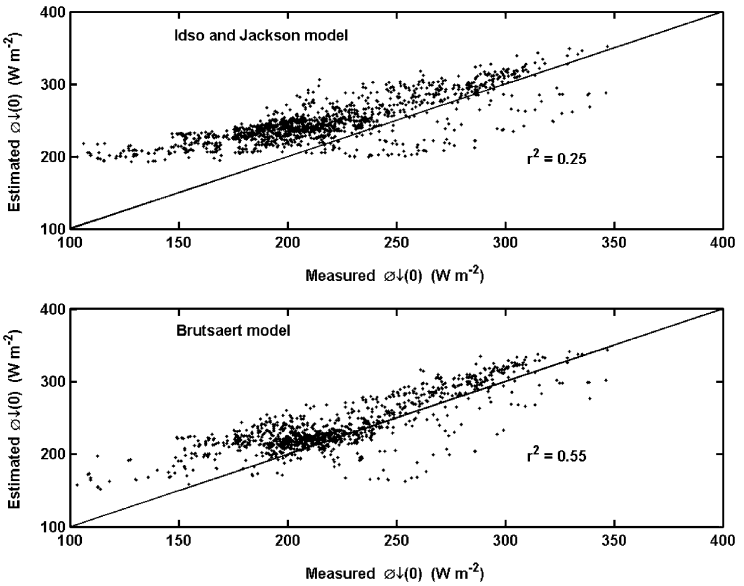

Fig. 5. Same as Fig. 4 but for the mountain site (1991–1994).

both sites accounts for the existence of a lower amount of water vapor at the mountain site relative to the lowland site.

4.2.2. Clear-sky condition: a new parameterization

This study presents a new parameterization for $\emptyset\downarrow(0)$ as follows:

$$\emptyset\downarrow(0) = \sigma T_a^4\{1 - X_s \exp(-Y_s e/T_a)\} \quad (5)$$

where $X_s = 0.35$, $Y_s = 10.0$ K hPa^{-1} for the lowland site and $X_s = 0.43$, $Y_s = 11.5$ K hPa^{-1} for the mountain site. In obtaining this parameterization, the entire hourly data for each of the lowland and mountain sites was split into two, with one half of the data set (i.e., 1991 data set for the lowland and 1991–1992 data set for the mountain site) being utilized for the modeling and the other half (i.e. 1992 data set for the lowland, 1993–1994 data set for the mountain site)

Table 4
Coefficients of Brunt's clear-sky atmospheric emissivity relation $\varepsilon_0 = A_4 + B_4 e^{(1/2)}$ as reported by various investigators and the overall variability

Investigator	Location	A_4	B_4 (hPa$^{-1/2}$)
Brunt (1932)—*Original work*	Benson (UK)	0.55	0.065
Monteith (1961)	Kew (UK)	0.53	0.065
Swinbank (1963)	Australia	0.64	0.037
Sellers (1965)	22 locations World-wide	0.61	0.048
Berger et al. (1984)	France	0.66	0.040
Berdahl and Martin (1984)	Six locations in U.S.A.	0.56	0.059
Heitor et al. (1991)	Lisbon (Portugal)	0.59	0.044
Present study	Bremgarten (Germany)	0.60	0.064
Present study	Feldberg (Germany)	0.50	0.066
Variability (%)	All the above locations	13	32

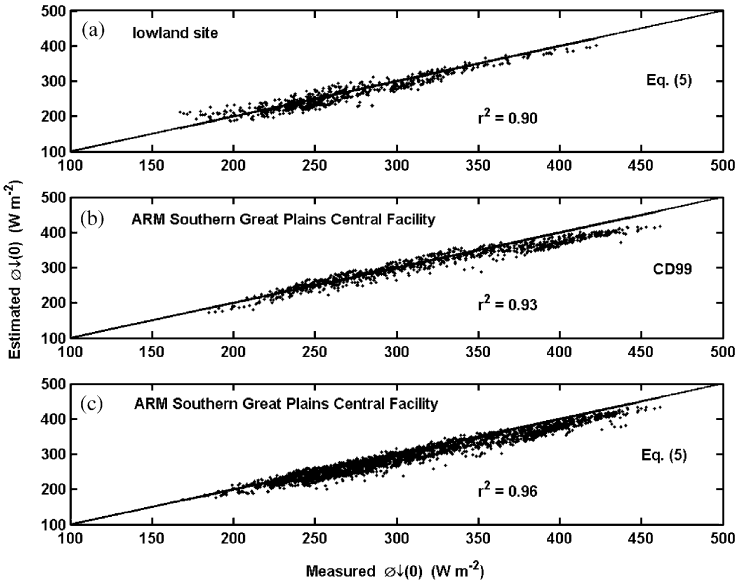

Fig. 6. (a) Hourly downward longwave clear-sky irradiance estimated from Eq. (5) versus measured irradiance at the study lowland site (1992); (b) hourly downward longwave clear-sky irradiance estimated from CD1999 (see text for details) versus measured irradiance at the ARM Southern Great Plain Central Facility (1998–1999) and (c) hourly downward longwave clear-sky irradiance estimated from Eq. (5) versus measured irradiance at the ARM Southern Great Plain Central Facility (1998–1999).

being used for the validation. The SE, NMBE and NRMSE of Ø↓(0) estimated using Eq. (5) were 14 W m^{-2}, −2% and 6%, respectively, for the lowland site, and 19 W m^{-2}, −1% and 9%, respectively, for the mountain site. Measured hourly values of Ø↓(0) and those estimated using Eq. (5) agreed within about 7% for the mountain site.

The U.S. Southern Great Plains Cloud and Radiation Testbed site is the first and the largest field measurement site, established by the Department of Energy's Atmospheric Radiation Measurement (ARM) Program. The heavily instrumented Central Facility (36.60° N, 97.50°W, 315 m a.s.l.) of the ARM site is located on a 65-ha cattle pasture and wheat fields southeast of Lamont, Oklahoma. As indicated in Section 1, Crawford and Duchon (1999) estimated daytime Ø↓ for the ARM site. In Fig. 6, we present a validation of Eq. (5) for the lowland site, while also comparing the performance of Eq. (5) with that of Crawford and Duchon (1999) (hereafter reffered to as CD99) for the ARM site. As for the study sites, the clear-sky observations at the ARM site were made by trained observers (Iziomon and Lohmann, 2003). Here we utilize 2 years (1998–1999) of hourly-averaged ARM clear-sky data. As shown in Fig. 6 (a and c), values of Ø↓(0) and those estimated using Eq. (5) agree within about 5% for both the lowland and ARM sites. It is

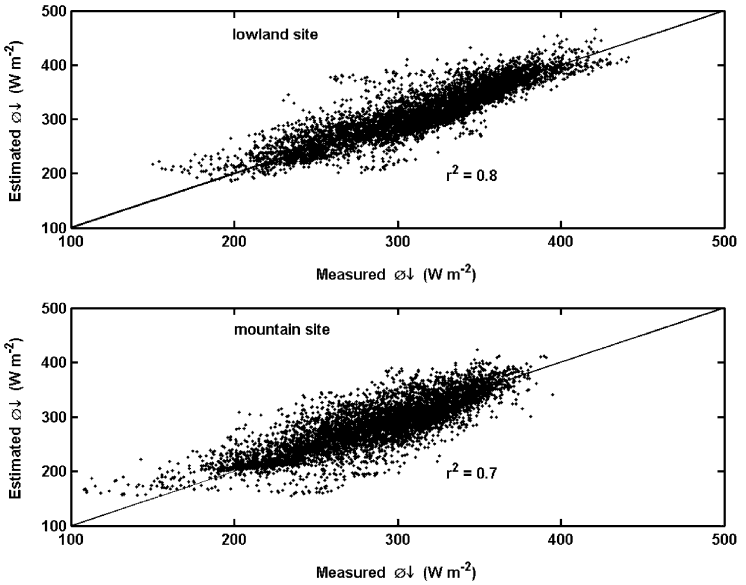

Fig. 7. Hourly downward longwave all-sky irradiance estimated from Eq. (6) versus measured irradiance at the lowland site (1992) {above} and mountain site (1993–1994) {below}.

Table 5
Model accuracy during various seasons

Season	Model accuracy for lowland site (%)		Model accuracy for mountain site (%)	
	Clear-sky model	All-sky model	Clear-sky model	All-sky model
Winter	6	8	6	9
Spring	4	5	5	8
Summer	4	5	4	6
Autumn	6	5	11	8

noteworthy that Eq. (5) gave higher regression coefficients, lower statistical errors and hence better estimates of $Ø\downarrow(0)$, compared to the other models examined in Section 4.2.1.

Furthermore, Eq. (5) and CD99 exhibited similar high performance. However, the fact that Eq. (5) yielded higher coefficient of determination (r^2) for the ARM site {see Fig. 6c} and is usable for both daytime and nighttime conditions, renders it more practicable than CD99, which can only be used to estimate $Ø\downarrow$ for daytime conditions.

4.2.3. All-sky conditions

The presence of cloud increases atmospheric irradiance received at the surface, since the radiation from water vapor and carbon dioxide in the lower atmosphere gets supplemented by emission from clouds in the waveband which the gaseous emission lacks. For application under cloudy sky conditions, the new clear-sky formulation therefore require appropriate modification. To parameterize $Ø\downarrow$ for all-sky conditions, measured hourly data covering one year (1991) for the lowland site and 2 years (1991–1992) for the mountain site were fitted to a relation of the form $Ø\downarrow(N) = Ø\downarrow(0)(1 + Z_sN^2)$ where Z_s is a coefficient. This method is justified by the fact that $Ø\downarrow$ varied approximately as N^2 at the study sites and that $Ø\downarrow = Ø\downarrow(0)$ when $N = 0$ okta. Substituting Eq. (5) for $Ø\downarrow(0)$, hourly downward atmospheric radiation for the lowland and mountain sites under variable sky conditions is given by

$$Ø\downarrow(N) = \sigma T_a^4\{1 - X_s \exp(-Y_s e/T_a)\}(1 + Z_sN^2) \qquad (6)$$

where e is in hPa, N is in okta, T_a is in K, $Z_s = 0.0035$ for the lowland site and $Z_s = 0.0050$ for the mountain site. Eq. (6) was validated using 1 year (1992) data set for the lowland site and 2 years (1993–1994) data set for the mountain site. Fig. 7 presents hourly values of measured $Ø\downarrow$ and those estimated for the lowland and mountain site using Eq. (6). In general, measured and estimated $Ø\downarrow$ agreed within 6% for the lowland site and 7% for the mountain site. The SE, NMBE and NRMSE of estimated $Ø\downarrow$ were

23 W m^{-2}, −1% and 7%, respectively, for the lowland site and 27 W m^{-2}, −0.5% and 9% for the mountain site.

Furthermore, the dependence of total effective atmospheric emissivity ε on cloudiness for the lowland site and mountain site can be approximated by

$$\varepsilon(N) = \varepsilon_0(1 + Z_s N^2), \quad (7)$$

where ε_0 averaged 0.78 and 0.70 for the lowland and mountain sites, respectively. The higher ε_0 obtained for the lowland site is consistent with higher air temperature and water vapor concentration at the site relative to the mountain site. In effect, it follows that clear-sky emissivity increases with water vapor mixing ratio but declined with altitude.

4.2.4. Comments on time scales and the applicability of proposed parameterization in climate models

As indicated in Sections 4.2.2 and 4.2.3, accuracies of 5–7% for hourly data of atmospheric downward irradiance are reported for the newly proposed parameterization. This range of accuracy is impressive and quite sufficient for some atmospheric applications. However for global climate applications, errors of ±5 W m^{-2} are desirable. On monthly and seasonal time scales, the errors reported here could be somewhat smaller. In particular, better accuracies are obtained during spring and summer months (see Table 5). As next steps, we plan to compare estimates of Ø↓ from various global climate models with those obtained from our parameterizations to determine the applicability of the latter in climate models.

5. Conclusion

Long-term data on atmospheric downward irradiance is still rare. This lack of data is even more pronounced for high grounds. Most existing models were developed based on short-term data (which were often collected from a lowland site) and for clear-sky conditions only. Based on a long-term data set, this study examines the downward atmospheric radiation budget and investigates models for its estimation, given clear and cloudy sky conditions at a lowland and a mountain location. The large difference in the elevation of the study sites results in a significant contrast in their climatology and hence their longwave radiation regime. Of the existing models evaluated here, Brutsaert and Brunt models performed better than the other ones. By yielding estimates, which agree with measured values within 5% for lowland and 7% for mountain locations, our newly proposed parameterization performed better than the other clear-sky models examined here. Furthermore, hourly downward all-sky irradiance estimated from our model yielded estimates, which agree with measurement within 6% for the lowland site and 7% for the mountain site. Since a realistic estimation of downward longwave irradiance is crucial to radiation balance investigations, the impressive long-term data set as well as the model evaluation presented here are pertinent to a range of atmospheric applications.

Acknowledgements

The sites used for this study were operated within the framework of a regional climate project (REKLIP) funded by the Ministry of Science and Research, Baden-Wuerttemberg, Germany. Thanks are due to the funding agency as well as to Prof. em. A. Kessler, Prof. Dr. L. Jaeger and Mr. W. Wicke for their participation in REKLIP on behalf of the Meteorological Institute, University of Freiburg, Germany. The Atmospheric Radiation Measurement (ARM) Program sponsored by the U.S. Department of Energy, Office of Science, Office of Biological and Environmental Research, Environmental Sciences Division, provided us with supporting data on downward atmospheric irradiance at the Southern Great Plain Central Facility, for which we are grateful. We also thank the Dalhousie University Killam Trust and the German Academic Exchange Service (DAAD) for supporting this study.

References

Alados-Arboledas, L., 1993. Estimation of hourly values of downward atmospheric radiation under cloudless skies during day- and night- time conditions. Theoretical and Applied Climatology 48, 127–131.

Ångström, A., 1918. A study of the radiation of the atmosphere. Smithsonian Institution Miscellaneous Collections 65, 159–161.

Badescu, V., 1997. Verification of some very simple clear and cloudy sky models to evaluate global solar irradiance. Solar Energy 61, 251–264.

Berdahl, P., Martin, M., 1984. Emissivity of clear skies. Solar Energy 32, 663–664.

Berger, X., Buriot, D., Garnier, F., 1984. About the equivalent radiative temperature for clear skies. Solar Energy 32, 725–733.

Bolz, H.M., Falkenberg, G., 1949. Neubestimmung der Konstanten der Ångströmschen Strahlungsformel. Z. Meteorologie 3, 97–100.

Brutsaert, W., 1975. On a derivable formula for long-wave radiation from clear skies. Water Resources Research 11, 742–744.

Brutsaert, W., 1982. Evaporation into the Atmosphere—Theory, History and Application. Kluwer Academic Publishers, Dordrecht.

Brunt, D., 1932. Notes on radiation in the atmosphere. Quarterly Journal of the Royal Meteorological Society 58, 389–418.

Chevallier, F., Cheruy, F., Armante, R., Stubenrauch, C.J., Scott, N.A., 2000. Retrieving the clear sky vertical longwave radiative budget from TOVS: comparison of a neural network-based retrieval and a method using geophysical parameters. Journal of Applied Meteorology 39, 1527–1542.

Crawford, T.M., Duchon, C.E., 1999. An improved parameterization for estimating effective atmospheric emissivity for use in calculating daytime downwelling longwave radiation. Journal of Applied Meteorology 38, 474–480.

Culf, A.D., Nash, J.H.C., 1993. Longwave radiation from clear skies in Niger: a comparison of observations with simple formulas. Journal of Applied Meteorology 32, 539–547.

Czeplak, G., Kasten, F., 1987. Parametrizierung der atmosphärischen Wärmestrahlung bei bewölktem Himmel. Meteorologische Rundschau 40, 184–187.

Davies, J.A., Mckay, D.C., Luciani, G., Abdel-Wahab, M., 1988. Validation of models for estimating solar radiation on horizontal surfaces, Vol. 1, IEA Task IX, Final Report. Atmospheric Environment Service of Canada, Downsview, Ontario, Canada.

DIN-VDI Handbook 333 (1999). Environmental meteorology, Meteorological measurements, Part 2—Global radiation, turbidity, visual weather observations, meteorological measuring stations for agric purposes. Beuth Verlag GmBH, Berlin. Wien. Zurich, 206 pp.

Festa, R., Ratto, C.F., 1993. Solar radiation statistical properties. Technical Report for IEA Task IX, University of Genova.

Garratt, J.R., Prata, A.J., 1996. Downwelling long-wave fluxes at continental surfaces—a comparison of observations with GCM simulations and implications for the global-land surface radiation budget. Journal of Climate 9, 646–655.

Heitor, A., Biga, A.J., Rosa, R., 1991. Thermal radiation components of the energy balance at the ground. Agricultural and Forest Meteorology 54, 29–48.

Idso, S.B., Jackson, R.D., 1969. Thermal radiation from the atmosphere. Journal of Geophysical Research 74, 5397–5403.

Intergovernmental Panel on Climate Change [IPCC], 2001. In: J.T. Houghton et al. (Eds.), Climate Change 2001: The Scientific Basis, Cambridge University Press, New York.

Iziomon, M.G., Lohmann, U., 2003. Optical and meteorological properties of smoke-dominated haze at the ARM Southern Great Plains central facility. Geophysical Research Letters 30, 1123. doi:10.1029/2002GLO16606.

Keding, I., 1989. Klimatologische Untersuchung über die atmosphärische Gegenstrahlung und Vergleich von Berechn ungsverfahren anhand langjähriger Messungen im Oberrheintal. Berichte des Deutschen Wetterdienstes, No. 178.

Kessler, A., Jaeger, L., 1999. Long-term changes in net radiation and its components above a pine forest and a grass surface in Germany. International Journal of Climatology 19, 211–226.

Llebot, J.E., Jorge, J., 1984. Some results of thermal atmospheric radiation measurements in Manresa (Spain). Solar Energy 32, 473–477.

Monteith, J.L., 1961. An empirical method for estimating long-wave radiation exchanges in the British Isles. Quarterly Journal of the Royal Meteorological Society 87, 171–179.

Prata, A.J., 1996. A new long-wave formula for estimating downward clear-sky radiations at the surface. Quarterly Journal of the Royal Meteorological Society 122, 1127–1151.

Sellers, W.D., 1965. Physical Climatology. University of Chicago Press, Chicago.

Swinbank, W.C., 1963. Long-wave radiation from clear skies. Quarterly Journal of the Royal Meteorological Society 89, 339–348.

Zhang, T., Stamnes, K., Bowling, S.A., 2001. Impact of the atmospheric thickness on the atmospheric downwelling longwave radiation and snowmelt under clear sky conditions in the Arctic and Subarctic. Journal of Climatology 14, 920–939.